coatings

MDPI

Article

Analysis and Control of Cracks in Ni60 Coating of 7050 Aluminum Alloy by Electron Beam Cladding

Hailang Liu *, Qian Zhang, Jian Chen, Zhuangji Zeng and Jie Tang

School of Mechanical and Electrical Engineering, Guilin University of Electronic Technology, Guilin 541004, China; 19012302073@mails.guet.edu.cn (Q.Z.); 19012201004@mails.guet.edu.cn (J.C.); 19012201002@mails.guet.edu.cn (Z.Z.); 20012302073@mails.guet.edu.cn (J.T.)
* Correspondence: liuhl@guet.edu.cn; Tel.: +86-137-6874-9062

Abstract: Ni60 electron beam cladding can play an important role in improving the properties of 7050 aluminum alloy. The cracking of the cladding layer, however, greatly affects the cladding quality. To solve this problem, the optimum range of cladding process parameters is determined by an experimental method: electron beam current [25–30 $\times$ 10^{-3} A], scanning speed [10–12 mm/s] and focusing current [700–720 $\times$ 10^{-3} A]. Through range analysis of the experiment results, the primary and secondary order of the influence of the cladding process parameters on the crack areal density is determined as follows: electron beam current > scanning speed > focusing current. A mathematical model of the crack areal density of the cladding layer is established based on the method of nonlinear regression, which is $y = 4.1553 \times 10^4\ I^{2.2887}\mathrm{V}^{-0.8379} {I_2}^{10.2675}$. It is shown that the model has obvious significance in the results of variance analysis, which can provide a basis for the selection of electron beam cladding process parameters.

Keywords: electron beam cladding; cladding crack; cladding process parameters

check for updates

Citation: Liu, H.; Zhang, Q.; Chen, J.; Zeng, Z.; Tang, J. Analysis and Control of Cracks in Ni60 Coating of 7050 Aluminum Alloy by Electron Beam Cladding. *Coatings* **2022**, *12*, 602. https://doi.org/10.3390/coatings12050602

Academic Editors: Panos Poulopoulos and Giorgos Skordaris

Received: 18 March 2022
Accepted: 27 April 2022
Published: 28 April 2022

Publisher's Note: MDPI stays neutral with regard to jurisdictional claims in published maps and institutional affiliations.

Copyright: © 2022 by the authors. Licensee MDPI, Basel, Switzerland. This article is an open access article distributed under the terms and conditions of the Creative Commons Attribution (CC BY) license (https://creativecommons.org/licenses/by/4.0/).

1. Introduction

Electron beam material surface cladding modification technology uses high-energy density electron beams to rapidly fuse the cladding material and the surface of the base material at the same time to form a modified surface with good metallurgical bonding; the surface of the base material forms a protective layer with good mechanical properties such as corrosion resistance, wear resistance, fatigue resistance and high-temperature resistance, which can give the material excellent surface properties [1,2].

7050 series aluminum alloy has good mechanical properties and is widely used in aircraft structures and high-strength and high-stress structures. However, these types of parts have strict requirements for material properties' not only must they have the characteristics of being light weight and high strength, but they also require very strong anti-flaking corrosion resistance and stress corrosion cracking resistance, fracture toughness and fatigue resistance. Although the strength and hardness of 7050 aluminum alloy can be improved through the conventional method of increasing the content of zinc and magnesium, its ability to resist stress corrosion and spalling corrosion will be reduced [3]. The Ni-based electron beam cladding layer has good heat resistance, fatigue resistance, stress corrosion resistance, anti-flaking corrosion resistance and oxidation resistance. If Ni-based material is cladded on the surface of 7050 aluminum alloy, its comprehensive mechanical properties can be improved. However, because the electron beam cladding process has the characteristics of fast-melting and solidification speed, it is easy to cause cracks in the Ni-based cladding layer, which affects the mechanical properties of the cladding parts, and even causes the parts to fail. Therefore, it is necessary to develop research on the cracks of the Ni-based cladding layer. ZHENG [4] prepared a Ni45 + TC4 cladding layer on the surface of a Ti811 alloy plate using laser cladding technology, and cracks appeared on the surface and the inside of the cladding layer. Li et al. [5] found

that Ni60 cracks originated on the top of the cladding layer and spread inward along the hard phase. The distribution of single-pass cladding cracks is relatively random, and the distribution of multi-pass cladding cracks has obvious directionality. In addition, toughness components are added to the powder, heat preservation and slow cooling during the cladding process, and lower input energy density can inhibit the occurrence of cracks. Yun et al. [6] added caf2-flux co-solvent powder to Cr_3C_2 powder when depositing Cr_3C_2 powder on the surface of AISi316l stainless steel material using electron beam irradiation to induce uniform melting of Cr_3C_2 powder and prevent cracking. Yu Bin et al. [7] used the method of optimizing the process parameters to control the cracks of the silicide coating. The study showed that a cladding layer without cracks can be obtained when the energy density of the electron beam is relatively small. However, the current research on crack control is mostly from the selection of cladding materials, pre-treatment before cladding, and auxiliary methods to reduce cracks, and there is a lack of in-depth research on the selection and optimization of cladding process parameters. In order to reduce the crack areal density of the 7050 aluminum alloy electron beam cladding Ni60 layer, ANSYS software is used to simulate the stress field of the 7050 aluminum alloy cladding Ni60 to narrow the range of process parameter selection of the orthogonal test method, reasonably arrange the combination of cladding process parameters for experiments, and analyze the extreme difference of the test results, obtain the order and influence trend of the influence of the process parameters on the crack areal density, and use nonlinear regression methods to establish the crack areal density equation and determine the preferred interval of the process parameters. It provides a theoretical basis for the selection of electron beam cladding process parameters.

2. ANSYS Temperature Field Simulation

The thermophysical parameters of powder coating materials and matrix materials have a great influence on the process of electron beam cladding. The thermophysical parameters in the numerical analysis of the temperature field during cladding are listed in Table 1. These parameters can be found in the literature [8]. However, most of them are at room temperature and change with the temperature during the cladding process. The thermophysical parameters at different temperatures can be obtained by JMatPro software.

Table 1. Thermophysical parameters of 7050 aluminum alloy and Ni60.

Material	Elastic Modulus/Pa	Poisson Ratio	Density/kg/m^3	Melting Poing/°C	Specific Heat Capacity/J/kg °C	Linear Expansion Coefficient/20 °C	Thermal Conductivity/W/m·k
7050	69×10^9	0.33	2830	488~635	860	23.5×10^{-6}	139.51
Ni60	206×10^9	0.3	8400	1040	456	18×10^{-6}	63

The quality of the electron beam cladding layer is closely related to its energy density input, and the energy density depends on the choice of process parameters. The range of values for the cladding process parameters is determined by ANSYS software simulation, which is aimed to find the process parameters that can make the temperature of the model above the melting point of the material, as well as make the temperature distribution reasonable. The intermediate point on the cladding path is selected as the research object in Figure 1, and when the simulation of the temperature field of the cladding process is completed, the temperature change curve of the specified point over time is going to be solved.

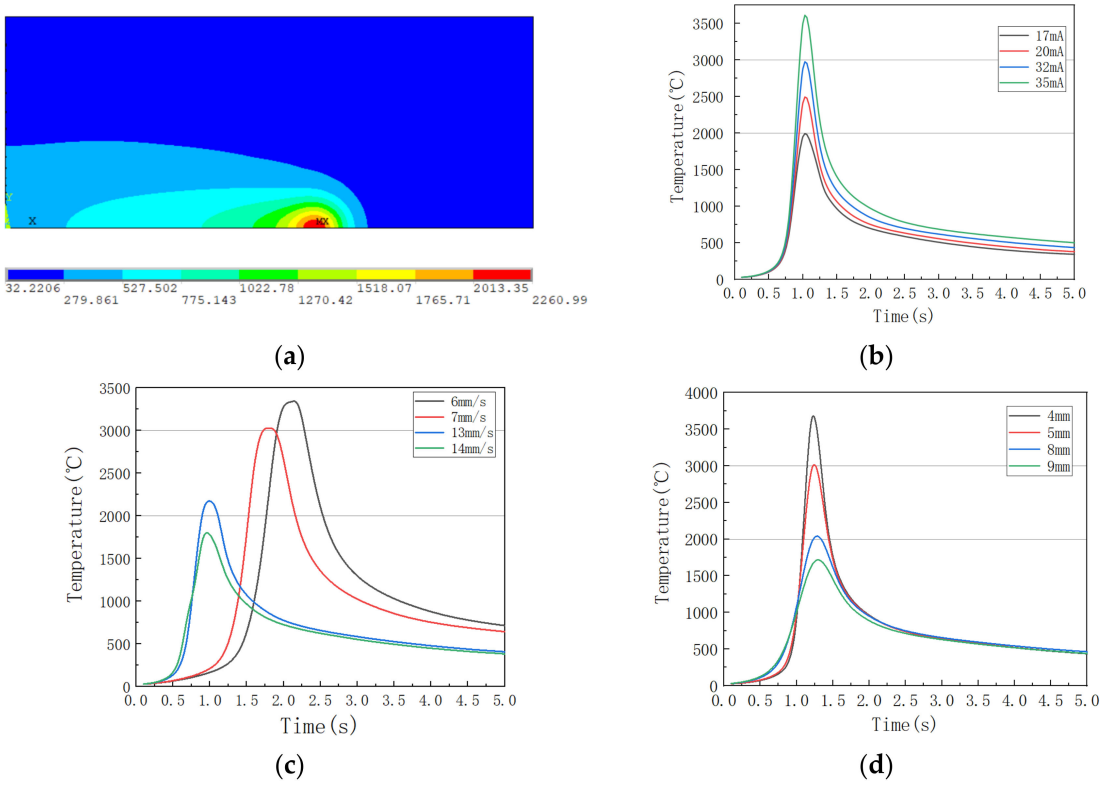


Figure 1. Temperature value range under different process parameters. (**a**) Temperature distribution of the melt pool. (**b**) Effect of electron beam flow on the melt pool temperature. (**c**) Effect of scanning speed on the melt pool. Temperature. (**d**) Effect of beam spot diameter on the melt pool temperature.

According to the melting point and thickness of the Ni60 powder coating, the reasonable value of the temperature at the surface study ranges from 2000 to 3000 °C. On the one hand, the temperature of this point is so low that the matrix and even the coating are not melted thus the combination strength is weak, resulting in the phenomenon of coating shedding; on the other hand, the phenomenon of the vaporization of the matrix over melting arose due to the temperature being too high. It can be seen from the curve in Figure 1b that when all parameters except the beam are kept constant, the temperature peak increases with the increase of the beam, and the beam is proportional to the peak temperature. When the beam is 17 mA, the peak temperature of the study point is lower than 2000 °C, and when the beam is 32 mA, the peak temperature of the study point is close to 3000 °C, so the reasonable value range of the beam is between 17 and 32 mA. From Figure 1c, it can be seen is that the larger the scanning speed, the smaller the temperature peak, and the scanning speed is inversely proportional to the peak temperature; when the scanning speed is 14 mm/s, the peak temperature of the study point is lower than 2000 °C, when it is 7 mm/s, the peak of the study point is about 3000 °C, so the reasonable value range of the scanning speed is between 7 and 13 mm/s. From Figure 1c, it can be seen that the diameter of the bundle is inversely proportional to the peak temperature, and the reasonable value range of the beam diameter (the beam diameter should be converted into focusing current during processing) is 5–8 mm.

3. Materials and Methods

The test base material is the plate of 7050 aluminum alloy, which is processed by wire cutting to a size of 50 mm × 20 mm × 10 mm. The cladding powder is Ni60, with a thickness of 1 mm. The chemical composition of the cladding powder Ni60 and the base material 7050 aluminum alloy are shown in Table 2.

Table 2. Elemental composition of powder material and matrix material.

Material wt%	**C**	**Si**	**Cr**	**B**	**Fe**	**Ni**				
Ni60	1.0	4.5	17	4.5	15	remainder				
Material wt%	**Si**	**Fe**	**Cu**	**Mn**	**Mg**	**Cr**	**Zn**	**Ti**	**Zr**	**Al**
7050	0.12	0.15	2.4	0.1	2.3	0.04	6.2	0.06	0.11	remainder

Many factors, such as accelerating voltage, electron beam current, focusing current, scanning speed, scanning waveform, preset powder thickness, overlap rate, and dilution rate, have a direct impact on the quality of the cladding layer. The main parameters that affect the crack areal density are electron beam current, scanning speed, and beam spot diameter.

The orthogonal experimental method can use reasonable experimental design methods and obtain certain data through experiments. Such an experimental design method can reduce the number of experiments a lot and can still represent the effect of full-factor experiments by designing a three-factor and three-level experimental program. The selected factors are current, scanning speed, and beam spot diameter. The experimental program is shown in Table 3.

Table 3. The cladding process parameter's factor level table.

Factor \ **Level**	**1**	**2**	**3**
Electron Beam Current/10^{-3} A	25	30	32
Scanning Speed/mm/s	8	10	12
Focusing Current/10^{-3} A	680	700	720

The test equipment is the SX-EBM electron beam cladding equipment made by Guilin Shichuang Vacuum Numerical Control Equipment Co., Ltd. (Guilin, China). The maximum voltage is 60 kV, the maximum power is 3 kW, the maximum scanning speed is 1000 mm/min, and the vacuum chamber vacuum is 5×10^{-2} pa. After the cladding was completed, a Leica confocal laser microscope DCM-3D was used to scan and analyze the microscopic surface cracks of the cladding layer.

According to the test plan on the orthogonal table, a Leica laser confocal microscope is used to scan the microsurface of the cladding layer of 7050 aluminum alloy. After that, Ni60 was cladded onto it with the electron beam, the cracks are shown in Figure 2. The purpose of this experiment was to analyze the influence of the process parameters on surface quality and use the crack areal density (ratio of crack area to detection area) to provide data for subsequent analysis. (In order to better reflect the cladding quality, the nine detection points are taken in places where cracks are prone; that is, at 45 mm of the scanning length). The processing technology in Figure 2 is shown in Table 4. The crack areal density in Table 4 is the crack detection results from Figure 2.

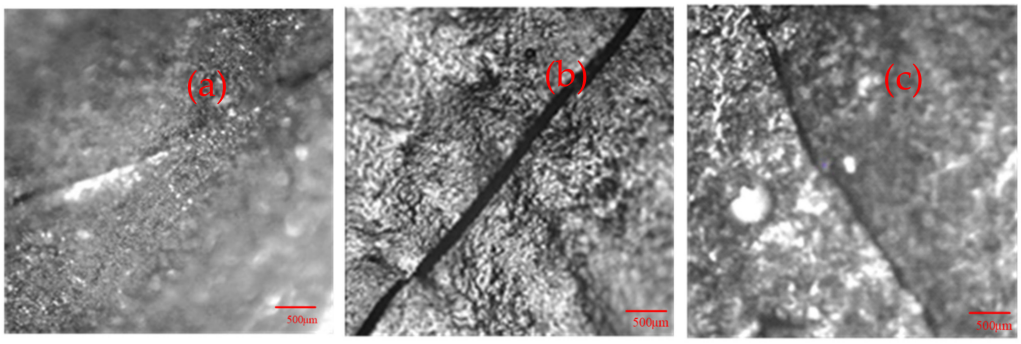


Figure 2. *Cont.*

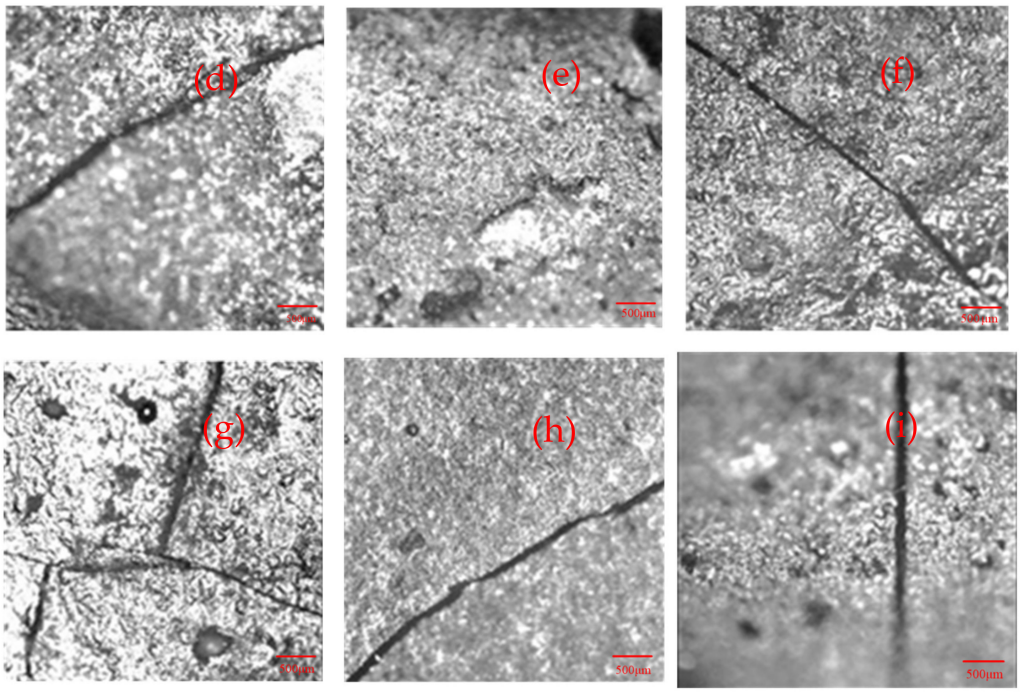


Figure 2. Picture of test crack.

Table 4. Results of orthogonal experiment scheme.

Number	Electron Beam Current/10^{-3} A	Scan Speed/mm/s	Focus Current/10^{-3} A	Crack Areal Density
a	25	8	680	0.007
b	25	10	700	0.032
c	25	12	720	0.012
d	30	8	720	0.014
e	30	10	680	0.003
f	30	12	700	0.016
g	32	8	680	0.061
h	32	10	720	0.031
i	32	12	700	0.021

4. Results, Discussion, and Analysis

4.1. Method for Dividing Optimization Interval of Process Parameters

The optimization interval of the process parameters is defined as the level interval of the process parameters with the least surface microcracks from the cladding process parameters. Selecting the cladding process parameters in this way can obtain a cladding layer with higher surface quality [9].

The method of dividing the optimal interval is based on the concepts as follows: (1) There are n process parameters (i.e., $N_1, N_2, \ldots, N_n$), and each process parameter has m levels (i.e., $M_1, M_2, \ldots, M_m$). To carry out the orthogonal test of the n factor and m level, we calculate the crack areal density range value based on the test results and determine the sensitivity of the crack areal density to various process parameters. (2) Calculating the average value of the crack areal density $\overline{I_i}$ (i is the corresponding column, $i = 1, 2, \ldots, n$) at each level (I, II, III ...) of sensitive process parameters; that is, the arithmetic average of the crack areal density when the factor on any column is at level i. (3) For the process parameter Ni, calculate the average value A_j of the crack areal density in $m - 1$ horizontal intervals $Q_j = [M_j, M_j + 1]$ and the range value R_j of the horizontal interval. (4) The process parameter level interval corresponding to the minimum average value min ($A_1, A_2, \ldots, A_j$) is the

optimal interval; if there are several optimal intervals, the optimal interval with the smallest extreme value among these several intervals is determined to be the optimal interval.

4.2. Analysis of Primary and Secondary Factors of Cladding Process Parameters

The range analysis of the crack areal density of the orthogonal test is carried out. I_i indicates the sum of the crack areal density corresponding to the level number of any column i; s is the number of occurrences of each factor level in any column; $\bar{I}_i$ is the arithmetic average of the crack areal density in any column. R is the range value $R = max(\bar{I}_i) - min(\bar{I}_i)$. The size of the range reflects the magnitude of the change in the result caused by the change of the process parameters in the range of values. The larger this value is, the greater the influence of the process parameter on the experimental results are; that is, the process parameter in the column with the largest range is the most important influencing factor. According to the test results, the range values of the cladding process parameters are calculated as shown in Table 4.

As can be seen from Table 5, the magnitude of the R-value of the process parameter determines the degree of influence of the parameter on the crack areal density, and the larger the R-value is, indicates that the parameter has a greater influence on the crack. In the selected parameter range, the degree of influence is: electron beam current > scanning speed > focusing current, in order. The electron beam current is the main influence factor for crack generation, and the variation of the value in the test range has the greatest influence on the crack; the variation of the value of the focusing current in the test range has the least influence on the crack.

Table 5. K value table of crack areal density.

Level \ Facror	Electron Beam Current/10^{-3} A	Scanning Speed/mm/s	Focus Current/10^{-3} A
1	0.0170	0.0273	0.0237
2	0.0110	0.0220	0.0230
3	0.0377	0.0163	0.0190
R	0.0267	0.0110	0.0047

4.3. Optimal Interval of Cladding Process Parameters

According to the second step of the optimal interval division method, the average value of the crack areal density is obtained when the three process parameters are taken at the three levels, respectively. The trend diagram of the influence of the factor level change on the crack is drawn in Figure 3.

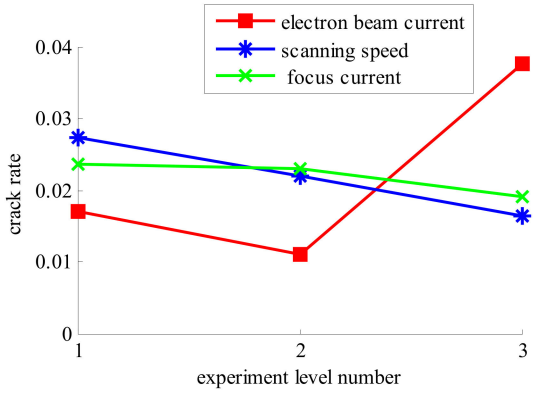
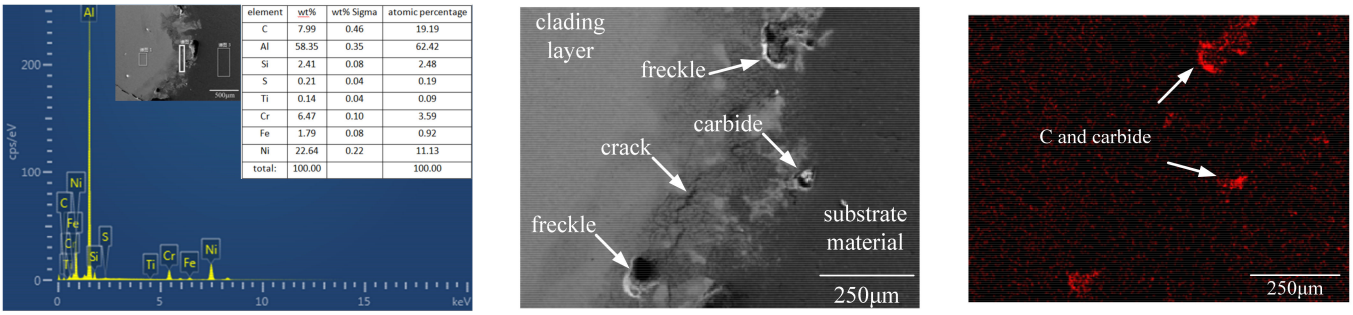


Figure 3. The influence of various factors on the R-value of the crack areal density.

It can be seen from Figure 3 that at the beginning, the cracks decrease with the increase of the electron beam current, and after the minimum value, the crack increases with the increase of the beam current. When the electron beam cladding starts, the substrate is at

room temperature, and the heat dissipation rate is fast. It is easy for Cr and C in Ni60 to accumulate and form hard, brittle phases during the non-equilibrium fusion process, and the cladding layer is very easy to crack. With the increase of the beam current and the increase of the substrate temperature, the cooling rate of the molten pool is reduced, which can inhibit the formation of Cr, C, and hard, brittle phases in the cladding layer, thereby blocking the initiation of cracks. When the beam current increases again, under the bombardment of a large number of high-energy electrons, the Ni60 powder coating and the surface of the 7050 substrate will melt and increase. Due to the low melting point of the aluminum alloy, vaporization and volatilization will occur on the surface, and the cracks in the bonding zone will increase. The analysis shows that the minimum average value of the crack areal density in the electron beam interval [25–30 $\times$ 10^{-3} A] is 0.01, and the variation range is 0.01–0.017. According to the method of determining the optimal interval, this interval is the optimal interval of the electron beam.

As shown in Figure 4, Ni60 powder contains a small amount of carbon. The addition of a small amount of carbon is beneficial in reducing the shrinkage of the alloy layer, inhibit the formation of freckles, and can reduce the chance of recrystallization. A proper amount of Cr can promote the formation of the TCP phase, thereby improving the stability of the structure. However, carbide-forming elements, such as Cr and C, are prone to segregation at the grain boundaries, and more carbide is precipitated. The precipitation of carbides requires Cr atoms to diffuse through grain boundaries and short-range lattice diffusion to produce segregation. Therefore, near the grain boundaries, the concentration of chromium decreases and the precipitation of carbides at the grain boundaries will cause chromium depletion near the grain boundaries, and the depletion of chromium will reduce the intergranular corrosion resistance of the cladding layer.



(**a**) (**b**) (**c**)

Figure 4. Energy spectrum and electron microscope images of the binding region. (**a**) Binding zone of EDS. (**b**) Cross-section of SEM. (**c**) C element.

Shrinkage cavities and freckles appear near the discontinuously precipitated carbon and carbides along the grain boundary. Shrinkage cavities and freckles are the sources of the cracks. The influence of trace element carbon on shrinkage cavities is very important. AL-Jarba [10] selected the third-generation nickel-based single crystal superalloy LMSX-1 to study and found that when the carbon content is less than 0.05%, as the carbon content increases, the volume fraction of shrinkage cavities decreases; when the carbon content reaches 0.05%, as the carbon content increases, the volume fraction of shrinkage cavities increases. The elements AL and Ti are the forming elements of the eutectic. During the solidification of the cladding layer, the elements AL and Ti are enriched in the interdendritic region, which makes the average density of the interdendritic liquid lower than that of the dendrite stem. 7050 aluminum alloy contains a small amount of Ti; when the temperature is higher than 807 °C, the carbide TiC is precipitated in the bonding zone, and the C is precipitated in the Ni60. The precipitation of carbon and carbide causes the bonding strength of the bonding zone to be torn.

It can be seen from Figure 3 and Table 6 that the crack areal density decreases with the increase of scanning speed and focusing current. The minimum average value of the crack areal density in the scanning speed of 10–12 mm/s is 0.0163, and the variation range is 0.0213–0.0163; that is, this interval is the preferred interval; the minimum average value of the crack areal density in the focus current [700–720 $\times$ 10^{-3} A] is 0.019, and the variation range is 0.023–0.019; that is, this interval is the preferred interval.

Table 6. Optimal interval of process parameters.

Process Parameters	Preferred Interval	Crack Areal Density
Electron beam current/10^{-3} A	[25, 30]	0.01~0.017
Scanning speed/mm/s	[10, 12]	0.0213~0.0163
Focus current/10^{-3} A	[700, 720]	0.023~0.019

Figure 1c shows the cladding temperature when other cladding process parameters are fixed, and only the scanning speed is changed, which conforms to the *Es* formula of electron beam radiation energy.

Based on the analysis mentioned above, it can be seen that the temperature level affects the crack areal density, and the electron beam energy determines the temperature level. The cladding process parameters conform to the electron beam radiant energy *Es* formula.

$$Es = P/DV \tag{1}$$

where P is the electron beam power, D is the beam spot diameter, and V is the scanning speed.

When the scanning speed and focusing current increase, the radiation energy of the electron beam acting on the powder decreases, the melting depth of the matrix decreases, and the dilution rate of the matrix material to the cladding layer decreases, which increases the hardness and corrosion resistance of the cladding layer, and the surface quality of the cladding layer is improved [11,12].

4.4. Modeling Analysis

In the electron beam cladding process, three process parameters have an effect on the crack areal density when they are changed. It is imperative to determine the law between process parameters and the crack areal density. The least-squares method is a mathematical optimization technique that finds the best matching function of the data by minimizing the sum of the squares of the errors. The goal is to obtain a model of the fitting function when the objective function is minimized.

From the above analysis, it is not difficult to find that there are nonlinear relationships between the crack and the three process parameters. It is difficult to describe accurately using the first-order mathematical model. Usually, the second-order or higher-order mathematical model is used to approximate the test results. Suppose the test result, i.e., crack areal density, is y, and the main factors that affect the result during the machining process are the electron beam current is I, the scanning speed is V, and the focus current is I_j. We can establish a nonlinear mathematical model as

$$y = kI^{\alpha}V^{\beta}{I_2}^{\gamma} \tag{2}$$

where y is the crack areal density, k is the coefficient, α is the exponent of the electron beam current I, β is the exponent of the scanning speed V, and γ is the exponent of the focusing current I_2.

In order to facilitate the calculation, take the logarithm of both sides of the Equation (2) to obtain

$$\lg y = \lg k + \alpha \lg I + \beta \lg V + \gamma \lg I_2 \tag{3}$$

Using the least-squares method to regression fit the test data in Table 1, the second-order mathematical model of 7050 aluminum alloy electron beam cladding Ni60 is obtained:

$$y = 4.1553 \times 10^4 I^{2.2887} V^{-0.8379} {I_2}^{10.2675} \quad (4)$$

It can be seen from fitting Equation (4) that the significant sequence of the influence of various factors (the base number is less than 1) on the crack is: electron beam current, scanning speed, and focusing current. It shows that the primary and secondary factors of the predictive fitting model are consistent with those of experimental extreme value analysis, and the model fits well.

Regression sum of squares and degrees of freedom

$$S_R = \sum_{j=1}^{9} (\hat{y}_j - \overline{y})^2 = 0.009706,\ f_R = 3 \quad (5)$$

Residual sum of squares and degrees of freedom

$$S_e = \sum_{j=1}^{9} (y_j - \hat{y}_j)^2 = 0.004353 \quad (6)$$

$$f_e = 9 - 1 - 3 = 5 \quad (7)$$

Therefore,

$$F = \frac{S_R / f_R}{S_e / f_e} = \frac{0.009706/3}{0.004353/5} = 3.7162 \quad (8)$$

Looking up the table, we can see that $F_{0.1}(3,5) = 3.62$, so $F_{0.1} > F_{0.1}(3,5)$, therefore, the regression equation is significant

This empirical formula shows that reducing the radiation energy of the electron beam (i.e., reducing the electron beam current and increasing the scanning speed and focusing current) will minimize the cracks in the cladding layer.

5. Conclusions

In this paper, the optimal interval and fitting model of the process parameters of Ni60 for 7050 aluminum alloy electron beam cladding are studied, and the following conclusions are obtained:

(1) ANSYS software is utilized to simulate the temperature field under different electron beam cladding process parameters to determine the value range of the process parameters.
(2) The primary and secondary order of the influence of the process parameters on the crack is determined by the range value of the test results.
(3) Analysis of the influence trend of process parameter level changes and interval changes on cracks is undertaken, and the process parameters for the least factors of crack areal density, the optimal interval, are determined.
(4) A prediction model for Ni60 crack areal density of 7050 aluminum alloy electron beam cladding is established, which has important guiding significance for the selection of subsequent processing parameters.
(5) *F*-test analysis of the fitted model can effectively predict the crack areal density of Ni60 in electron beam cladding of 7050 aluminum alloy.

Author Contributions: Q.Z. was responsible for experiments and data processing and writing and revising papers. J.C. guided the revision of the thesis and also recommended and provided funding projects. H.L. helped solve experimental problems and provided project and fund support. Z.Z. assisted in translation, formal analysis, visualization, and review. J.T. helped with experimental questions, translation, and review. All authors have read and agreed to the published version of the manuscript.

Funding: This work was supported in part by the National Natural Science Foundation of China (NSFC) under Grant 51965012.

Institutional Review Board Statement: Not applicable.

Informed Consent Statement: Not applicable.

Data Availability Statement: No new data were created or analyzed in this study. Data sharing is not applicable to this article.

Conflicts of Interest: The authors declare no conflict of interest.

References

1. Oh, J.C.; Yun, E.; Golkovski, M.G.; Lee, S. Improvement of hardness and wear resistance in SiC/Ti-6Al-4V surface composites fabricated by high-energy electron beam irradiation. *Mater. Sci. Eng. A* **2003**, *351*, 98–108. [CrossRef]
2. Segura, I.A.; Murr, L.E.; Terrazas, C.A.; Bermudez, D.; Mireles, J.; Injeti, V.S.V.; Li, K.; Yu, B.; Misra, R.D.K.; Wicker, R.B. Grain boundary and microstructure engineering of Inconel 690 cladding on stainless-steel 316L using electron-beam powder bed fusion additive manufacturing. *J. Mater. Sci. Technol.* **2019**, *35*, 351–367. [CrossRef]
3. Dixit, M.; Mishra, R.S.; Sankaran, K.K. Structure–property correlations in Al 7050 and Al 7055 high-strength aluminum alloys. *Mater. Sci. Eng. A* **2008**, *478*, 163–172. [CrossRef]
4. Zheng, C. Research on the crack mechanism of laser cladding layer of nickel-based alloy. *China Met. Bull.* **2018**, *11*, 75–76. (In Chinese)
5. Li, Q.; Li, T.; Wu, Z.; Shi, B.; Zhang, H. Research on the crack mechanism of laser cladding layer of Ni-based alloy. *J. Dalian Univ. Technol.* **2020**, *60*, 159–164. (In Chinese)
6. Yun, E.; Lee, S. Correlation of microstructure with hardness and wear resistance in Cr 3 C 2/stainless steel surface composites fabricated by high-energy electron beam irradiation. *Mater. Sci. Eng. A* **2005**, *405*, 163–172. [CrossRef]
7. Yu, B.; Jin, Q.; Liu, Z.; He, J. Electron beam remelting surface modification technology of silicide coating. *Chin. Space Sci. Technol.* **2010**, *30*, 54–58. (In Chinese)
8. Lu, Q.; Du, C.; Wang, H.; Wang, C. Experimental study on the preparation of Ni60-based ceramic cladding by plasma spray welding of hot forging die. *Therm. Process. Process.* **2014**, *43*, 131–133. (In Chinese)
9. Zhang, J.; Wang, Z.; Zhao, L.; Liu, D.; Zhao, M. Laser cladding 4J36 low-expansion alloy coating process optimization based on orthogonal experiment method. *Ordnance Mater. Sci. Eng.* **2016**, *39*, 11–15. (In Chinese) [CrossRef]
10. Al-Jarba, K.A.; Fuchs, G.E. Effect of carbon additions on the as-cast microstructure and defect formation of a single crystal Ni-based superalloy. *Mater. Sci. Eng. A* **2004**, *373*, 255–267. [CrossRef]
11. Pogrebnjak, A.D.; Kravchenko, Y.A. Modification of mechanical properties of TiN/Al2O3and TiN/Cr/Al2O3coatings using low-energy high-current electron beams. *J. Superhard Mater.* **2013**, *35*, 105–110. [CrossRef]
12. Komizo, Y.; Taka, T.; Koso, M. Surface modification by high energy density beams. *Sumitomo Met.* **1990**, *42*, 157–164.